Supporting Information

Multifunctional Liquid Crystal Polymer Network Soft Actuators

*Li Yu, Ran Peng, Geoffrey Rivers, Che Zhang, Pengxiang Si and Boxin Zhao**

Prof. Li Yu,† Dr. Geoffrey Rivers, Che Zhang, Pengxiang Si, Prof. Boxin Zhao,
Department of Chemical Engineering, Waterloo Institute for Nanotechnology, Institute for Polymer Research, Centre of Bioengineering and Biotechnology, 200 University Avenue West Waterloo, ON, N2L 3G1, Canada
E-mail: zhaob@uwaterloo.ca

Prof. Li Yu,†
Hubei Collaborative Innovation Center for Advanced Organic Chemical Materials, Key Laboratory for the Green Preparation and Application of Functional Materials, Ministry of Education, Hubei Key Laboratory of Polymer Materials, School of Materials Science and Engineering, Hubei University, Wuhan 430062, China.

Dr. Ran Peng,†
Department of Mechanical and Industrial Engineering, University of Toronto, ON, M5S 3G8, Canada

† These authors contributed equally to this work.

SI-1: Fabrication of LCN tubular actuators

Fabrication of polydomain LCN tubes: For fabricating LCN tubular actuators, RM82 (HCCH Company), pentaerythritol tetrakis(3-mercaptopropionate) (PETMP) (Sigma-Aldrich), dipropyl amine (DPA) (Sigma-Aldrich), 2,2-dimethoxy-2-phenylacetophenone (DEAP) (Sigma-Aldrich) were selected as LC monomer, crosslinker, Michael-addition catalyst, and photo curing agent, respectively (**Figure S1a**). Typical procedure for synthesizing polydomain LCN tubes was as follows. RM82 (269.2 mg, 0.4 mmol), PETMP (97.8 mg, 0.2 mmol) and DEAP (7.5 mg) were firstly dissolved in 1.5 ml N,N´-dimethylformamide (DMF) solution and ultrasonicated for 5min. Then, a mixture solution containing all reagents were formed by adding 0.5 ml DMF solution containing DPA (6 mg) into above well mixed

solution. Finally, mixture solution containing all reagents was filled into a home-made mold made up of a cylinder and tube. Polydomain LCN tubes were obtained by completely evaporating DMF in vacuum oven at 80 ^{o}C for 24 hours. The dimension of polydomain LCN tubes such as its inner diameter was able to be controlled by devising the dimensions of the molds (**Figure S1b**).

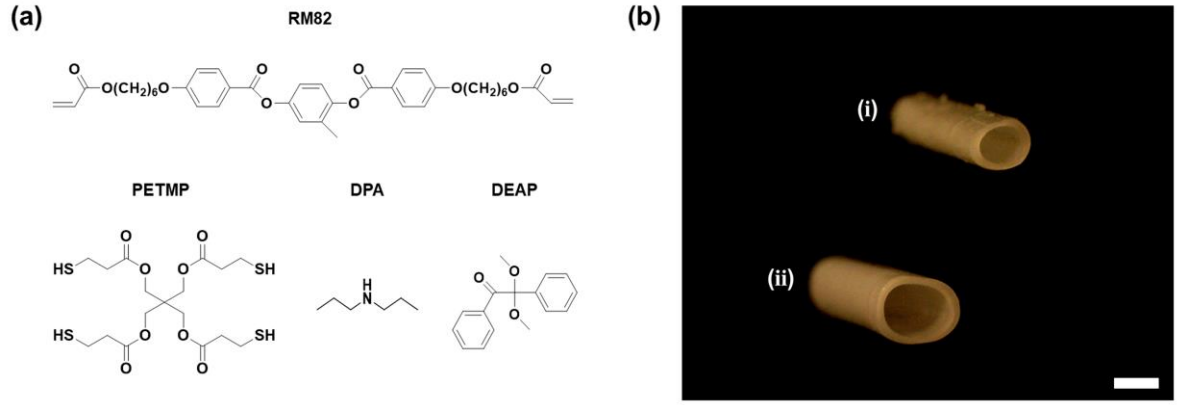

Figure S1. (a) Chemical structure the compounds for synthesizing LCN tubular actuators. (b) Photos of polydomain LCN tubes with different inner diameters. The scale bar is 1 mm.

Fabrication of LCN tubular actuators: Monodomain LCN tubes with uniaxial orientation along the length were achieved by mechanically stretching polydomain LCN tubes to the strain of 200%. After UV curing (30 mW/cm^2) for 30 min, LCN tubular actuators with reversible thermal-responsive shape changing behaviors were obtained.

SI-2: Nematic-to-isotropic transition temperature of LCNs

For determining stimulating temperature, we characterize polydomain LCNs using a Dynamic Mechanical Analyzer (Q800). The test was conducted in tension mode ranging from -40 ^{o}C to 280 ^{o}C at the frequency of 1 Hz. As presented in **Figure S2**, the nematic-isotropic phase transition temperature (T_{NI}) is around 135 ^{o}C.[1]

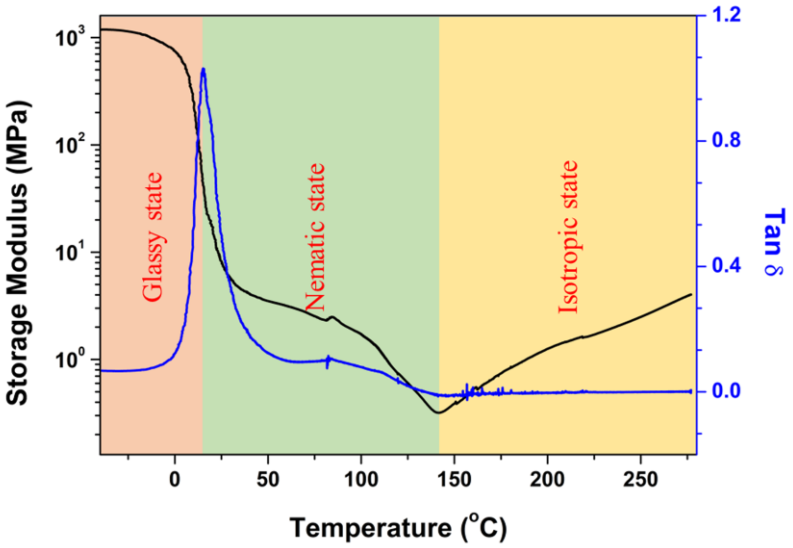

Figure S2. Storage modulus (E´) and loss tangent (tan δ) curves of polydomain LCNs measured at 3 °C/min heating (cooling) rate and 1 Hz frequency in the tension mode.

SI-3: Thermal stability of LCNs

We chose T = 250 °C as stimulating temperature because it is much higher than T_{NI} providing large reversible strain. Moreover, stimulating temperature T = 250 °C is much lower than the degradation temperature T = 340 °C guaranteeing stable thermal actuation behavior of LCN tubes (**Figure S3**).

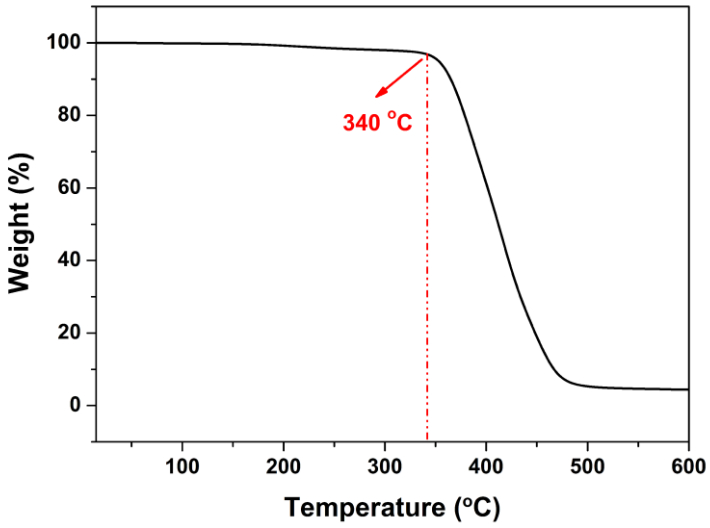

Figure S3. Thermogravimetric analysis curve of polydomain LCNs at air atmosphere.

SI-4: Orientation of LCs in LCN tubular actuators

In order to characterize the degree of LC orientation in LCN tubular actuators, defined as order parameter *S*, 2D-WAXD experiment was performed on a Bruker D8 Discover diffractometer with a 2D detector of GADDS in transmission mode. The 2D-WXRD patterns of polydomain and monodomain LCN tubes are shown in **Figure 1biii** and **iv**. Azimuthal intensity scan of the X-ray diffraction patterns of polydomain and monodomain LCN tubes are presented in **Figure S4**. The order parameter *S* is calculated based on Hermans-Stein orientation distribution function, where the I is the intensity and ϕ is the azimuthal angle as shown in **Figure S4**.

$$S = \frac{3\langle \cos^2 \phi \rangle - 1}{2}$$

$$\langle \cos^2 \phi \rangle = \frac{\int_0^{\pi/2} I(\phi) \sin\phi \cos^2 \phi d\phi}{\int_0^{\pi/2} I(\phi) \sin\phi d\phi}$$

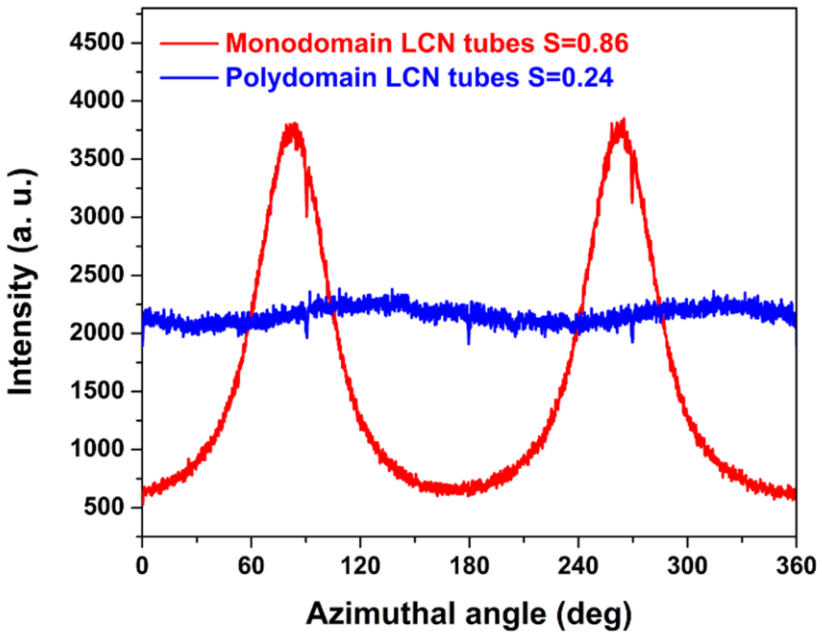

Figure S4. Azimuthal intensity scan of the X-ray diffraction patterns of polydomain and monodomain LCN tubes.

SI-5: Simulation of the change of inner diameter of LCN tubes during the process of the MPGP

Physical model and boundary conditions: The finite element modeling for evaluating the change of inner diameter of LCN tubes in the MPGP was conducted based on Comsol 5.3 with Solid Mechanics Module working with hyperplastic material. In the simulation, LCN tubes with height H_0 of 10 mm, inner radius R_0 of 1.3 mm, and outer radius R_1 of 1.8 mm were used as original model and subjected to a total elongation ΔH of 20 mm. As LCN tubes exhibit 2D axial symmetry, the model was further simplified to the rectangle (yellow area)

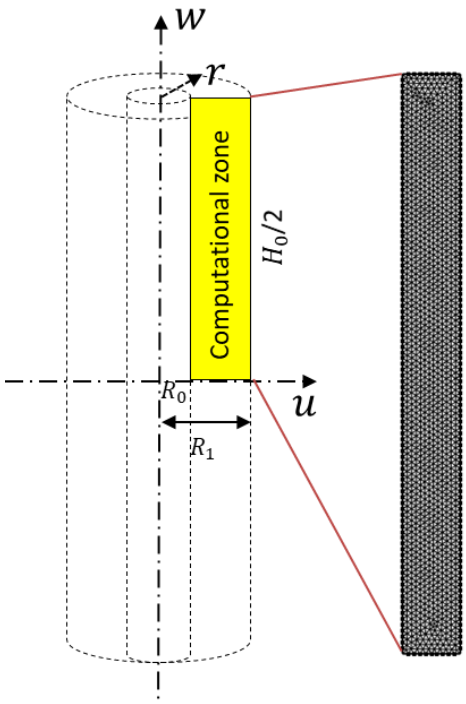

Figure S5. Schematic illustration the model for the simulation.

where the width was the thickness of LCN tubes and height was half of their initial length (**Figure S5**). The working parameters for the finite element modeling were obtained by fitting experimental data in the strain-stress curve of polydomain LCN tubes using MCalibration (VERST) software (**Figure 2a**). The governing equations are listed as follows:

$$\nabla \cdot \boldsymbol{FS} + \boldsymbol{F_v} = \boldsymbol{0},\ \boldsymbol{F} = \boldsymbol{I} + \nabla \boldsymbol{u} \qquad \textbf{Equation (S1)}$$

$$\boldsymbol{S} = \boldsymbol{S}_{ext} + \frac{\partial \boldsymbol{W}_s}{\partial \varepsilon},\ \sigma = \boldsymbol{J}^{-1}\boldsymbol{F}\boldsymbol{S}\boldsymbol{F}^T,\ \boldsymbol{J} = \det(\boldsymbol{F}) \qquad \textbf{Equation (S2)}$$

$$\varepsilon = \frac{1}{2}(\boldsymbol{F}^T\boldsymbol{F} - \boldsymbol{I}) \qquad \textbf{Equation (S3)}$$

where $\boldsymbol{u}$ is the displacement field, F is the applied force, ε is strain tensor, σ is the stress tensor. The boundary conditions for the displacement in the radical and axial directions u and w are as follows

$$w(r, 0) = 0 \qquad \textbf{Equation (S4)}$$

$$u(0, z) = 0 \qquad \textbf{Equation (S5)}$$

where r and z are radical and axial coordinate, the tensile strain is imposed through the top boundary with a prescribed elongation of $\Delta H = 10\ mm$.

$$w(r, H_0/2) = \Delta H \qquad \textbf{Equation (S6)}$$

$$u(r, H_0/2) = 0 \qquad \textbf{Equation (S7)}$$

Material model: As mentioned above, elastic behavior of LCN tubes was obtained by the tensile test and experimental strain-stress relation was applied to evalute the performance of polydomain LCN tubes. The strain-stress relation of polydomain was further calibrated by MCalibration software *via* curve fitting to match the 5-Parameter Mooney-Rivlin Hyperelastic model and the strain energy density can be obtained as follows

$$\boldsymbol{Ws} = C_{10} * (I_{1s} - 3) + C_{01} * (I_{2s} - 3) + C_{20} * (I_{1s} - 3)^2 + C_{11} * (I_{1s} - 3) * (I_{2s} - 3) + C_{02} * (I_{2s} - 3)^2 + (J - 1)^2/d$$

Equation (S8)

where $\boldsymbol{Ws}$ is the strain energy density, C_{10}, C_{01}, C_{20}, C_{11}, C_{02} are material constants and d is the incompressibility (initial bulk modulus factor) of the LCN material. All these constants are fitted and optimized by MCalibration software, as shown in **Table S1**. During our

experiment, the specimen experienced a very large strain (>500%), however, in this part, strain below 200% was simulated for our specific practical applications. The computational domain was meshed by 2606 elements with 12280 degrees of freedoms, as shown in **Figure S5**.

Table S1. Material constants of LCN tube obtained by Mcalibration.

Name	Value
C10	0.200112
C01	0.101718
C20	0.0115886
C11	-0.0461202
C02	-0.00750376
d	0.000388459

SI-6: Mechanical property of LCN tubular actuators

For the sake of evaluating the performance and stability of LCN tubular actuators as soft grippers, tensile test was carried out by a universal materials tester (UMT, UNMT-2MT) with a constant loading rate of 1 mm/s at room temperature about 22℃. As presented in **Figure S6**, the failure stress LCN tubular actuators is as high as 55 Mpa. In addition, the large failure strain of 138 % ensure that LCN tubular actuators would not break when contracting to wrap grasping objects.

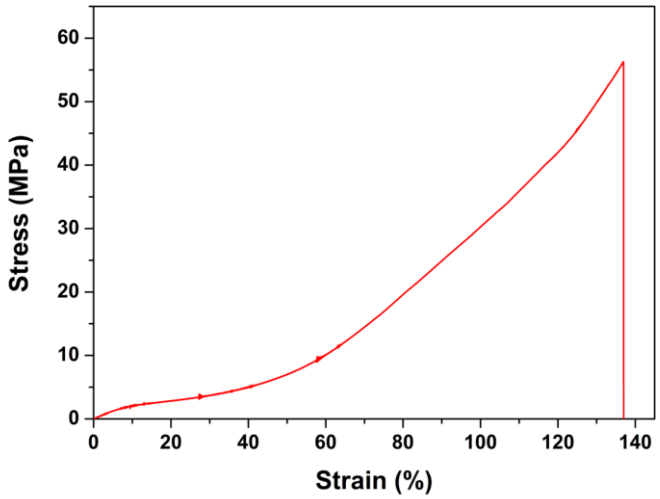

Figure S6. Stress-strain curve of LCN tubular actuators.

SI-7: Thermomechanical property of LCN tubular actuators

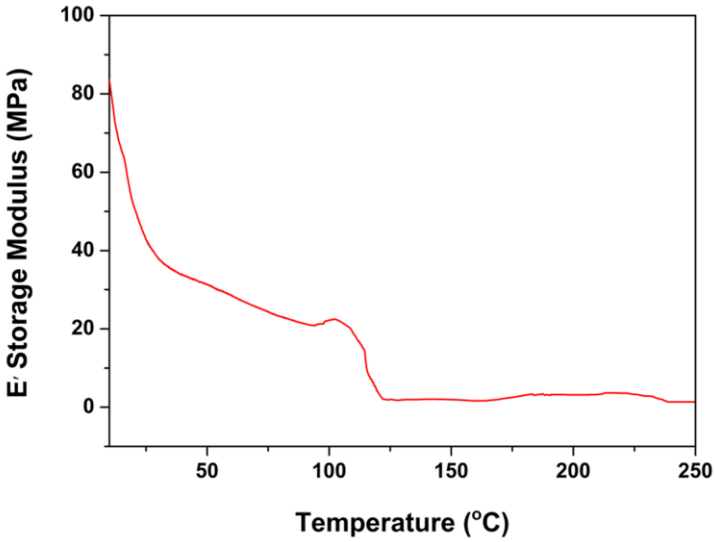

Figure S7. The temperature dependent curve for the storage modulus of LCN tubular actuators.

In order to characterize the load of LCN tubular actuators employed as a gripper, the storage modulus of LCN tubular actuators was measured using a Dynamic Mechanical Analyzer (Q800). The test was conducted in tension mode ranging from 0 °C to 250 °C at the frequency of 1 Hz. As shown in **Figure S7**, the storage modulus of LCN tubular actuators is 48 MPa at room temperature around 22 °C. In our work, the process of using LCN tubular actuators for

grabbing the objectives is performed at room temperature. On the contrary, the grabbing process for the only reported LCN tubular gripper is conducted as 100 ^{o}C with the storage modulus about 2 MPa.[2] Thus, our designed LCN tubular actuators can tolerate much higher load.

References

[1] M. O. Saed, A. H. Torbati, C. A. Starr, R. Visvanathan, N. A. Clark, C. M. Yakachi, *J. Polym. Sci. Part B: Polym. Phys.* **2017**, *55*, 157.

[2] X. J. Qian, Q. M. Chen, Y. Yang, Y. S. Xu, Z. Li, Z. H. Wang, Y. H. Wu, Y. Wei, Y. Ji, *Adv. Mater*. **2018**, 1801103.

Movie S1. Reversible thermal-responsive shape changing behaviors of LCN tubular actuators.

Movie S2. Simulated change of inner diameter of polydomain LCN tubes by mechanical stretching in the MPGP.

Movie S3. The outflowing of LMs from the syringe at room temperature.

Movie S4. Reversible thermal-responsive shape changing behaviors of multifunctional LM/LCN soft actuators.

Movie S5. Application of multifunctional LM/LCN soft actuators as thermal-responsive electrical switches.